


Original Research

# Shionone Alleviates Sepsis-Induced Acute Lung Injury by Regulating Macrophage Polarization Through the HMGB1/NF- $\kappa$ B Pathway

Qian Wu<sup>1,†</sup>, Geying Xi<sup>1,†</sup>, Ying Lin<sup>2</sup>, Junkai Zhao<sup>2</sup>, Yi Song<sup>1</sup>, Huojun Jiang<sup>1</sup>,  
Biao Zhang<sup>1,2,3,\*</sup> <sup>1</sup>Department of Critical Care Medicine, Suzhou Hospital of Integrated Traditional Chinese and Western Medicine, 215101 Suzhou, Jiangsu, China<sup>2</sup>Department of Emergency, Suzhou Hospital of Integrated Traditional Chinese and Western Medicine, 215101 Suzhou, Jiangsu, China<sup>3</sup>Department of Central Laboratory, Suzhou Hospital of Integrated Traditional Chinese and Western Medicine, 215101 Suzhou, Jiangsu, China\*Correspondence: [zhangbmed@126.com](mailto:zhangbmed@126.com) (Biao Zhang)

†These authors contributed equally.

Academic Editor: Jacek Kubiak

Submitted: 13 December 2025 Revised: 25 February 2026 Accepted: 28 February 2026 Published: 22 April 2026

## Abstract

**Background:** Sepsis-induced acute lung injury (ALI) poses a significant therapeutic challenge due to the lack of effective treatments. Shionone (SHI), a compound known for its anti-inflammatory properties, was investigated for its potential to mitigate ALI by modulating macrophage polarization, a key process in the inflammatory response. The underlying mechanism was also explored. **Methods:** We established lipopolysaccharide (LPS)-induced models of ALI in mice and RAW264.7 cells. The protective effects of SHI were assessed *in vivo* using lung histopathology (hematoxylin and eosin [H&E] staining) and the lung wet-to-dry weight ratio. Cell viability was assessed using a Cell Counting Kit-8 (CCK-8) assay. The levels of inflammatory cytokines (interleukin-6 [IL-6], interleukin-1 beta [IL-1 $\beta$ ], tumor necrosis factor-alpha [TNF- $\alpha$ ], granulocyte-macrophage colony-stimulating factor [GM-CSF], Interleukin-10 [IL-10], transforming growth factor-beta 1 [TGF- $\beta$ 1]) and polarization markers (inducible nitric oxide synthase [iNOS], arginase-1 [Arg1]) were quantified by enzyme-linked immunosorbent assay [ELISA] and real-time quantitative PCR. The expression of key proteins in the high-mobility group box 1 (HMGB1)/nuclear factor  $\kappa$  B (NF- $\kappa$ B) pathway (HMGB1, toll-like receptor 4 [TLR4], myeloid differentiation primary response 88 [MyD88], NF- $\kappa$ B p65) was analyzed by western blot and immunofluorescence. The study used a small interfering RNA [siRNA] loss-of-function strategy to demonstrate that HMGB1 is a critical target of SHI. **Results:** SHI treatment significantly attenuated sepsis-induced ALI in mice, as evidenced by improved lung histology, lower lung injury scores, and reduced pulmonary edema. In both *in vivo* and *in vitro* models, SHI suppressed the production of pro-inflammatory cytokines (TNF- $\alpha$ , IL-6, IL-1 $\beta$ ) and the M1 macrophage marker iNOS, while enhancing the release of anti-inflammatory cytokines (GM-CSF, IL-10, TGF- $\beta$ 1) and the M2 marker Arg1. Mechanistically, SHI inhibited the activation of the HMGB1/NF- $\kappa$ B pathway by downregulating the expression of HMGB1, TLR4, MyD88, and NF- $\kappa$ B phosphorylation. The critical role of HMGB1 was further supported by the finding that siRNA-mediated knockdown of HMGB1 mimicked the anti-inflammatory and polarization-shifting effects induced by SHI. **Conclusion:** Our findings demonstrate that SHI alleviates sepsis-induced ALI by reprogramming macrophage polarization from a pro-inflammatory M1 phenotype to an anti-inflammatory M2 phenotype. This protective effect is primarily mediated through the inhibition of the HMGB1/NF- $\kappa$ B signaling pathway. Thus, SHI represents a potential therapeutic candidate for sepsis-associated lung injury.

**Keywords:** acute respiratory distress syndrome; shionone; molecular mechanism; macrophage polarization; HMGB1; traditional Chinese medicine

## 1. Introduction

Acute lung injury (ALI) is a principal complication arising from sepsis [1]. Macrophage polarization, a key process in the development of sepsis, can lead to systemic decompensation, and exacerbate the inflammatory response, and have widespread effect during the development of sepsis. ALI involves dysregulated inflammation with an imbalance in macrophage polarization at its core. Excessive pro-inflammatory M1 macrophage activity promotes tissue damage, while deficient anti-inflammatory M2 macrophage function impairs repair. The specific signaling pathways governing this imbalance remain unclear, but elucidating these mechanisms is crucial for developing thera-

pies to modulate macrophage responses and improve ALI outcomes [2]. *Aster* is a traditional medicine used to treat ALI, with shionone (SHI) as its main active component. Previous studies have reported that SHI improves ALI [3].

Macrophages, as central nodes of immune activity, exhibit strong plasticity and versatility in response to changes in the body's internal environment. Under different stimulation conditions, macrophages can polarize into two distinct phenotypes: M1 (pro-inflammatory) and M2 (anti-inflammatory), which play opposing roles in inflammation, M1 pro-inflammatory type and M2 anti-inflammatory type, which play different roles in inflammation. Their polarization functions are almost antagonistic. M1 macrophages, induced by lipopolysaccha-



ride (LPS), release pro-inflammatory mediators, including interleukin-6 (IL-6), interleukin-1 beta (IL-1 $\beta$ ), tumor necrosis factor-alpha (TNF- $\alpha$ ) [4,5], and are characterized by the biomarker inducible nitric oxide synthase (iNOS). The M1 phenotype is known to aggravate inflammatory dysfunction. Conversely, M2 macrophages release anti-inflammatory cytokines interleukin-10 (IL-10), granulocyte-macrophage colony-stimulating factor (GM-CSF), transforming growth factor-beta 1 (TGF- $\beta$ 1) [5], and can be identified by arginase-1 (Arg1) [6]. Macrophage polarization is a complex process regulated by various signaling molecules and pathways. During ALI, ineffective control of the M1-dominated inflammatory immune response can lead to progression to ARDS [7]. Therefore, studying macrophage polarization is crucial for understanding the transformation between M1 and M2 macrophages and for developing treatments for inflammatory diseases. In-depth study of macrophage polarization mechanisms is essential to finding treatments for acute lung injury.

LPS activates nuclear factor  $\kappa$  B (NF- $\kappa$ B) and regulates M1 phenotype macrophage activation [8]. High-mobility group box 1 (HMGB1) is highly expressed in macrophages and plays a key role in inflammatory diseases. Studying HMGB1 as a target for anti-inflammatory therapy is significant [9,10]. Several studies have shown that HMGB1 can bind to toll-like receptors, activate NF- $\kappa$ B signaling and promote inflammatory response. It can also form complexes with other inflammatory factors, such as LPS and IL-1 $\beta$  to initiate inflammatory cascades [11–13]. HMGB1 inhibits GM-CSF and enhances phosphorylation of signal transducers and NF- $\kappa$ B [14], highlighting its crucial role in the NF- $\kappa$ B—related pathway.

The Chinese herbal medicine *Aster* exhibits a protective effect against respiratory diseases such as pharyngitis, cough, and asthma. Shionone, the primary active ingredient extracted from *Aster*, possesses antiviral and immunomodulatory properties. Previous study has reported that SHI can improve ALI and inhibit the expression of inflammatory factors, potentially through the regulation of macrophage polarization [3]. SHI exerts anti-inflammatory effects through the NF- $\kappa$ B pathway [15]. This study explores the mechanism by which shionone modulates M1/M2 macrophage polarization to alleviate LPS-induced acute lung injury.

## 2. Materials and Methods

### 2.1 Reagents

SHI was purchased from Yuanye Bio-Technology (B21703, Shanghai, China) and was solubilized in 0.1% (w/v) DMSO. LPS was obtained from Sigma (L4516, St. Louis, United States). Dexamethasone (DXM) was purchased from Chenxin Drug Store (H37021969, Jining, China).

### 2.2 Animals

Male C57BL/6 mice (8 weeks old) were obtained from Jihui Co., Ltd. (Shanghai, China). The mice were housed in a standard laboratory environment maintained a temperature of  $24 \pm 1$  °C, humidity of 40–60%, and a 12 h light/dark cycle. The mice were allowed to acclimatize to these conditions for one week before the start of the experiment. All experimental procedures were performed in accordance with the NIH Guide for the Care and Use of Laboratory Animals, and were based on established literature [8]. All efforts were made to minimize the number of animals used and their suffering. Each group consisted of three or more animals. For our study, anesthesia was induced in mice using inhaled isoflurane (3–4%) and maintained at 1.5–2% prior to euthanasia. The euthanasia method consisted of a two-step procedure compliant with the AVMA Guidelines (2020): first, a deep overdose with  $\geq 5\%$  isoflurane for over five minutes post-respiratory arrest, followed immediately by cervical dislocation as a confirmatory physical method to ensure death. All procedures were approved by our Institutional Animal Care and Use Committee (No.2023032). The mice were randomly assigned to five groups: control, LPS, LPS+DXM (5 mg/kg), LPS+SHI-L (50 mg/kg), and LPS+SHI-H (100 mg/kg). A murine sepsis model was induced by intraperitoneal injection of LPS. Drug administration was performed via intragastric gavage 2 hours before LPS injection, and again at 0, 2, and 12 hours post-injection. The mice were euthanized by inhalation of an overdose of anesthetic agent. Lung tissues were then collected and processed as follows: one portion was used to determine the wet-to-dry weight ratio, another portion was fixed in 4% paraformaldehyde was purchased from Servicebio (G1101, Wuhan, China), and the remaining samples were stored at  $-80$  °C.

### 2.3 Lung Wet-to-Dry Weight Ratio

The lungs were removed from the sacrificed mice and weighed to obtain the wet weight (W). The lung tissues were then dried at 65 °C for 48 hours and weighed again to obtain the dry weight (D). The wet-to-dry weight (W/D) ratio was calculated to assess the degree of pulmonary edema.

### 2.4 Histopathological Analysis/Hematoxylin and Eosin Staining and Lung Injury Score

Lung tissues were fixed in 4% paraformaldehyde, embedded in paraffin, and sectioned. After deparaffinization and rehydration, the sections were stained with hematoxylin and eosin (H&E). Pulmonary histopathological changes were observed under a CX53 microscope (Olympus, Tokyo, Japan). Lung injury scoring was performed by an experienced investigator blinded to the treatment groups (categorized as absent, mild, moderate, or severe with scores ranging from 0 to 3). The assessment was based on the presence of exudates, hyperemia, congestion, neutrophilic infiltration, intra-alveolar hemorrhage, debris, and cellular

**Table 1. Murine primer sequences for qRT-PCR.**

Primer name	Forward (5' to 3')	Reverse (5' to 3')
$\beta$ -actin	GTGCTATGTTGCTCTAGACTTCG	ATGCCACAGGATTCCATACC
High-mobility group box 1	AGGCTGACAAGGCTCGTTATGAAAG	GGGCGGTACTIONCAGAACAACAAG
inducible nitric oxide synthase	ATCTTGGAGCGAGTTGTGGATTGTC	TAGGTGAGGGCTTGGCTGAGTG
Arginase-1	AGACAGCAGAGGAGGTGAAGAGTAC	TGAGTCCGAAGCAAGCCAAGG
Transforming growth factor-beta 1	CAACAATTCCTGGCGTTACCTTGG	TGTATTCCGTCTCCTTGGTTCAGC
Interleukin-10	TGGACAACATACTGCTAACCGACTC	GCCGCATCCTGAGGGTCTTC
Granulocyte-macrophage colony-stimulating factor	CCAGGAGATTCCACAACACTCAGGTAG	TGAGAGGCTGTAGACCACAATGC
Interleukin-1 beta	TACAGGCTCCGAGATGAACAAC	TGCCGTCTTTCATTACACAGGA
Interleukin-6	AGCCAGATCCTTCAGAGAGA	TGGTATTGGTCTTAGCCAC
Tumor necrosis factor-alpha	CACAGAAAGCATGATCCGCG	ACTGATGAGAGGGAGGCCAT

hyperplasia. Each of the following indicators was scored on a 0–4 scale: edema, atelectasis, necrosis, alveolar and interstitial inflammation, hemorrhage, and hyaline membrane formation. The scoring criteria were defined as follows: 0 = no injury; 1 = 25% injury; 2 = 50% injury; 3 = 75% injury; 4 = 100% injury. For each slide, the score of each injury indicator was evaluated in 10 randomly selected fields at 200 $\times$  magnification [16].

### 2.5 Cell Culture

Murine RAW264.7 macrophage cells were obtained from iCell (Shanghai, China) and were cultured in Dulbecco's Modified Eagle Medium supplemented with 10% heat-inactivated fetal bovine serum. Cells were maintained in a 37 °C incubator with a humidified atmosphere of 5% CO<sub>2</sub> and 95% air. Subculturing was performed every 1–2 days, and only cells in the logarithmic growth phase were used for experiments. Cells were seeded into six-well or 96-well plates at a density of 5  $\times$  10<sup>3</sup> cells/mL and incubated for 24-hour before the culture medium was replaced. The RAW264.7 cells were divided into four groups: control, LPS, LPS+SHI-L (2  $\mu$ g/mL), and LPS+SHI-H (4  $\mu$ g/mL). Cells were pretreated with SHI at concentrations of 2.0  $\mu$ g/mL (SHI-L) and 4.0  $\mu$ g/mL (SHI-H) for 2 hours, then stimulated with LPS (5  $\mu$ g/mL) for 24 hours. Cell supernatants and cells were then collected for subsequent experimental analyses. All cell lines were validated by STR profiling and tested negative for mycoplasma.

### 2.6 Transfection

HMGB1-siRNA was obtained from Hippobiotec Co., Ltd. (Huzhou, China). For cell preparation, 1  $\times$  10<sup>5</sup> cells were inoculated in 400  $\mu$ L of antibody free medium one day before transfection to ensure 50% cell confluence. For transfection, siRNA was diluted with 50  $\mu$ L Opti-MEM to a final concentration of 50 nM and gently pipetted 3–5 times to mix. The transfection reagent, Lipofectamine 2000, was gently mixed by inversion before use. Then, 1.2  $\mu$ L of Lipofectamine 2000 was diluted in 50  $\mu$ L of Opti-MEM, gently pipetted (3–5 times) to mix thoroughly, and incubated at room temperature for 5 minutes.

The transfection reagent mixture was combined with the siRNA diluent via gentle pipetting (3–5 times) and allowed to stand at room temperature for 20 minutes. The transfection complex was added to the 24-well cell plate, and the plate was gently shaken back and forth to mix evenly. Cell culture plates were incubated in a 5% CO<sub>2</sub> incubator at 37 °C for 48 hours. Fresh medium was replaced 4–6 hours after transfection. RAW264.7 cells were divided into the following groups: control, LPS, HMGB1-siRNA (knockdown), LPS+HMGB1-siRNA, LPS+SHI, and LPS+HMGB1-siRNA+SHI. Cells were first treated with SHI at a concentration of 2.0  $\mu$ g/mL for 2 hours, followed by stimulation with LPS for 24 hours [8].

### 2.7 Quantitative Real-Time Polymerase Chain Reaction

Total RNA was isolated from cells using the MolPure Cell/Tissue Total RNA Kit (Yeasen 19221ES50, Shanghai, China). Reverse transcription was performed using with the HiScript II Q RT SuperMix Kit (Vazyme R223-01, Nanjing, China). Quantitative real-time PCR (qRT-PCR) was then performed using SYBR qPCR Master Mix (Medical-bio MR0321, Suzhou, China) according to the manufacturer's protocols. The 20  $\mu$ L reaction system consisted of 1  $\mu$ L cDNA template, 0.4  $\mu$ L each of forward and reverse primers, 10  $\mu$ L SYBR Premix Ex Taq, and 8.2  $\mu$ L ddH<sub>2</sub>O.  $\beta$ -actin was used as the internal reference gene, with primer sequences detailed in Table 1 (Sangon Biotech, Shanghai, China). Relative mRNA expression levels were calculated using the 2<sup>− $\Delta\Delta$ CT</sup> method.

### 2.8 Enzyme-Linked Immunosorbent Assay (ELISA)

The concentrations of IL-1 $\beta$ , IL-6, TNF- $\alpha$ , IL-10, TGF- $\beta$ 1 and GM-CSF, were measured using commercial ELISA kits according to the manufacturer's instruction (MultiSciences EK201, EK206, EK282, EK210, EK981, EK263, Hangzhou China). The concentrations of HMGB1 were determined using commercial ELISA kits (Qiaoyi JEN-018, Hefei, China) in accordance with the manufacturer's instructions.

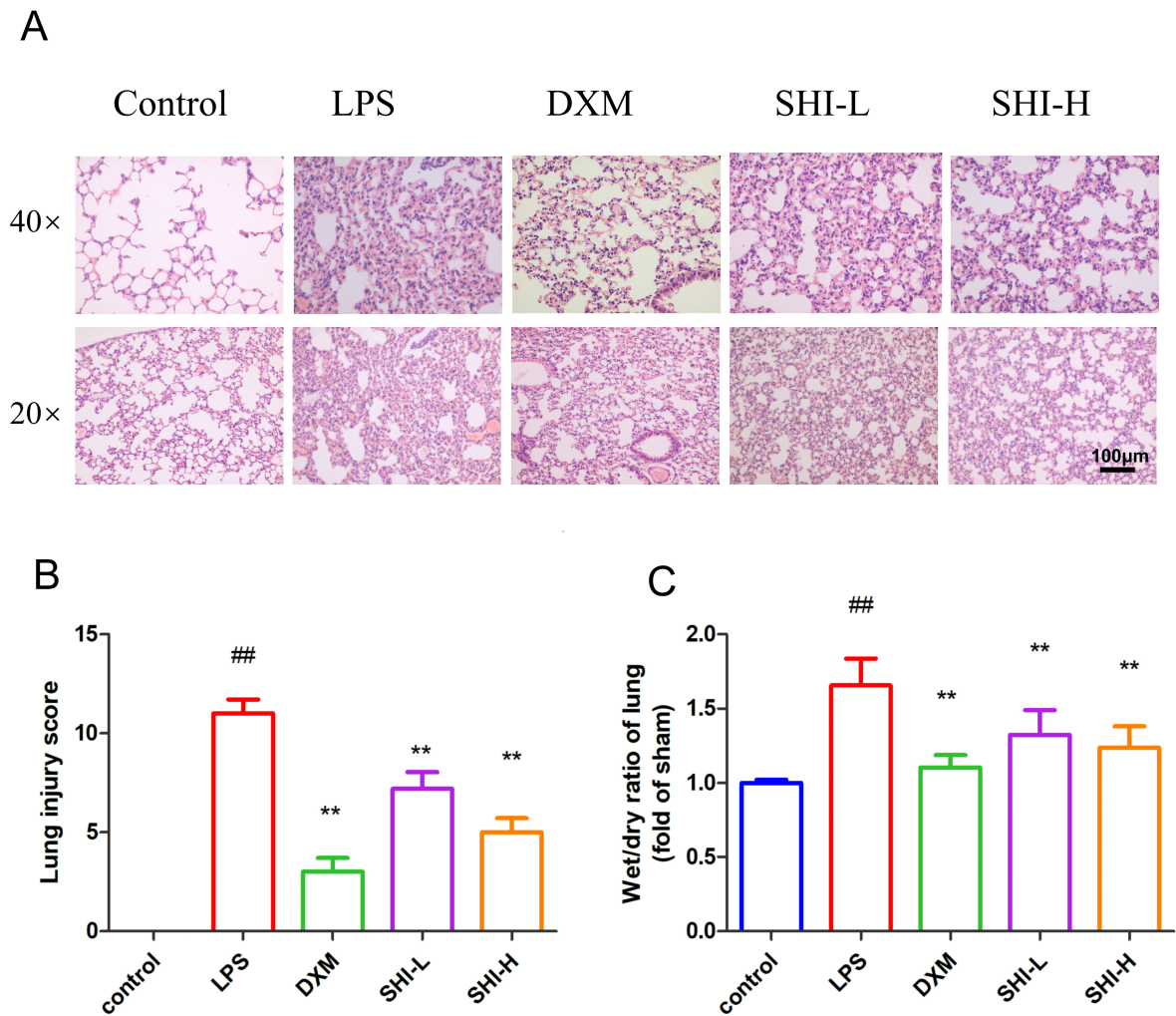


**Fig. 1. SHI ameliorated LPS-induced ALI *in vivo*.** (A) The histopathological alteration by H&E staining. Scale bar: 100 µm. (B) The lung injury score. (C) The wet-to-dry ratio of the lungs. Compared with the control group,  $##p < 0.01$ , compared with the LPS group,  $**p < 0.01$ . SHI, Shionone; LPS, lipopolysaccharide; ALI, acute lung injury; H&E, hematoxylin and eosin; DXM, dexamethasone; L, low; H, high.

### 2.9 Western Blot

Proteins were extracted from RAW264.7 cells using radio immunoprecipitation assay (RIPA) buffer (Beyotime P0038, Shanghai, China), and their concentrations were measured with a BCA kit (Beyotime P0009, Shanghai, China). After denaturation, equal protein loads were resolved on 8–12% SDS-PAGE gels and electrotransferred to PVDF membranes. Following a 1-hour block in 3% bovine serum albumin (Servicebio GC305010, Wuhan, China), membranes were probed with specific primary antibodies overnight at 4 °C. Primary antibodies against HMGB1 (ZenBio R22773 1:3000, Chengdu, China), p-NF- $\kappa$ B (ZenBio 310013 1:1000, Chengdu, China), NF- $\kappa$ B (ZenBio 380172 1:1000, Chengdu, China), MyD88 (ZenBio 340629 1:1000, Chengdu, China), TLR4 (ZenBio 505258 1:1000, Chengdu, China), iNOS (ZenBio 340668 1:1000, Chengdu, China), Arg1 (Proteintech 16001-1-AP 1:10,000, Wuhan, China), and  $\beta$ -actin (ZenBio R380624 1:7500, Chengdu,

China). Subsequently, membranes were washed, incubated with HRP-conjugated secondary antibodies (Zenbio 511203 1:7500, Chengdu, China) for 1 hours, and the signals were visualized via enhanced chemiluminescence.

### 2.10 Immunofluorescence Staining

Cells were fixed with 4% paraformaldehyde, then permeabilized and blocked with 3% BSA containing 0.1% Triton X-100. The cells were then incubated overnight at 4 °C with an anti-Arg1 primary antibody. After thorough washing, cells were incubated with an Alexa Fluor® 488-conjugated secondary antibody for 1 hour in the dark at room temperature. Nuclei were counterstained with 4',6-diamidino-2-phenylindole (DAPI) for 10 seconds. Finally, samples were mounted with an anti-fade mounting medium (Beyotime, Shanghai, China) and visualized under a CX53 microscope (Olympus, Tokyo, Japan). Fluorescence intensity was quantified using ImageJ software 2.1.4.7 (National

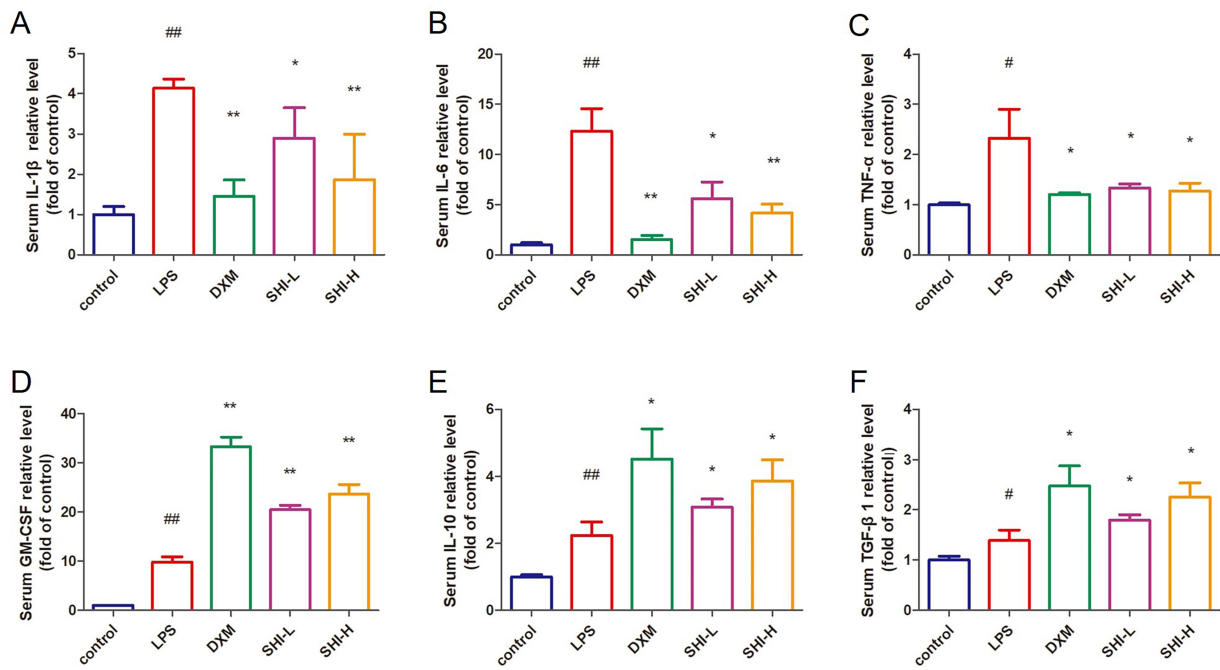


**Fig. 2.** SHI inhibited the expression of serum inflammatory factors in ALI models. (A–F) IL-1 $\beta$ , IL-6, TNF- $\alpha$ , GM-CSF, IL-10 and TGF- $\beta$ 1 expression in the serum. Compared with the control group, # $p < 0.05$ , ## $p < 0.01$ , compared with the LPS group, \* $p < 0.05$ , \*\* $p < 0.01$ .

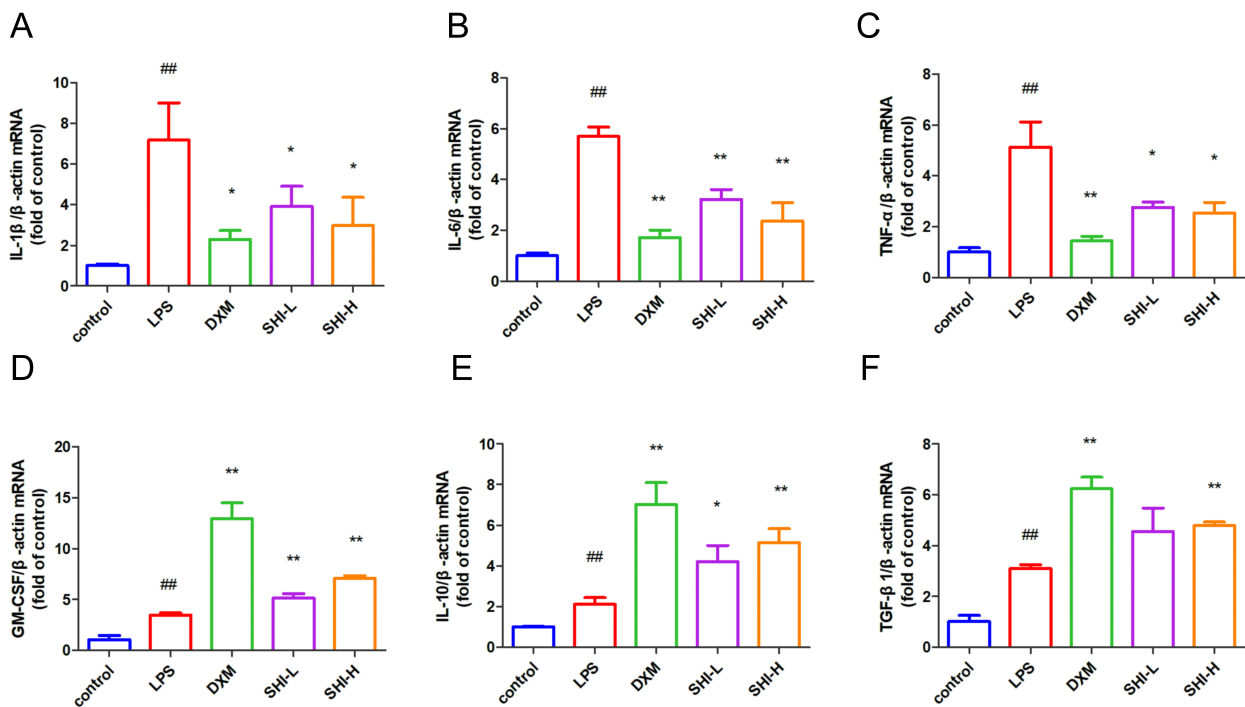


**Fig. 3.** SHI inhibited the expression of inflammatory factors in ALI model lung tissue. (A–F) IL-1 $\beta$ , IL-6, TNF- $\alpha$ , GM-CSF, IL-10 and TGF- $\beta$ 1 expression in the lung tissues by mRNA. Compared with the control group, ## $p < 0.01$ , compared with the LPS group, \* $p < 0.05$ , \*\* $p < 0.01$ .

Institutes of Health, Bethesda, MD, USA), and representative images were captured.

### 2.11 Statistical Analysis

Data are expressed as mean  $\pm$  SEM. All experiments were independently repeated at least three times. Statistical

analyses were performed using GraphPad Prism 8 software (GraphPad Software, Boston, MA, USA). For comparisons among three or more groups, one-way analysis of variance (ANOVA) was used followed by Tukey's honestly significant difference (HSD) post hoc test for pairwise comparisons when variances were equal.

### 3. Results

#### 3.1 SHI Improved LPS-Induced ALI In Vivo

Our findings indicate that SHI can mitigate ALI in LPS-induced septic mice. Histopathological changes were evaluated via H&E staining. As shown in Fig. 1A, LPS challenge induced characteristic pathological features including inflammatory cell infiltration, pulmonary edema, and alveolar wall thickening. Treatment with SHI (100 mg/kg) or DXM markedly attenuated these changes, whereas SHI at 50 mg/kg showed a lesser effect (Fig. 1A). Additionally, SHI significantly improved the lung injury score (Fig. 1B). The LPS group exhibited a significantly elevated wet-to-dry weight ratio compared to the control group ( $p < 0.01$ ). In contrast, treatment with SHI and DXM markedly reduced the pulmonary wet-to-dry weight ratio relative to the LPS group ( $p < 0.01$ ) (Fig. 1C).

#### 3.2 SHI inhibited the Expression of Serum Inflammatory Factors in ALI Models

LPS stimulation significantly increased serum levels of IL-1 $\beta$ , IL-6, and TNF- $\alpha$  ( $p < 0.05$ ). Both SHI and DXM treatments significantly decreased these serum levels ( $p < 0.05$ ) (Fig. 2A–C). Compared to the LPS group, the relative levels of GM-CSF, IL-10, and TGF- $\beta$ 1 in the serum of SHI and DXM groups were significantly increased ( $p < 0.05$ ) (Fig. 2D–F). A higher dose SHI (100 mg/kg) exhibited a stronger effect than a lower dose SHI (50 mg/kg). Compared to the control group, LPS stimulation increased the expression of IL-1 $\beta$ , IL-6, TNF- $\alpha$ , GM-CSF, IL-10, and TGF- $\beta$ 1 ( $p < 0.05$ ) (Fig. 2).

#### 3.3 SHI Inhibited the Expression of Inflammatory Factors in ALI Lung Tissue

The mRNA levels of IL-1 $\beta$ , IL-6, and TNF- $\alpha$  in lung tissue of mice stimulated by LPS were significantly increased ( $p < 0.05$ ). Both SHI and DXM interventions significantly reduced these mRNA levels ( $p < 0.05$ ) (Fig. 3A–C). Compared with the LPS group, the relative mRNA levels of GM-CSF, IL-10, and TGF- $\beta$ 1 in lung tissues of SHI and DXM groups were significantly increased ( $p < 0.05$ ) (Fig. 3D–F). A higher dose of SHI (100 mg/kg) appeared to have a stronger effect than a lower dose of SHI (50 mg/kg). Compared with the control group, LPS stimulation increased the mRNA expressions of IL-1 $\beta$ , IL-6, TNF- $\alpha$ , GM-CSF, IL-10, and TGF- $\beta$ 1 ( $p < 0.05$ ) (Fig. 3).

#### 3.4 SHI Affects Macrophages Polarization and HMGB1 Expression in ALI Model

The expression of the polarization markers iNOS and Arg1 mRNA was examined in the lung tissues of mice stimulated by LPS for 24 hours. The results showed that the iNOS mRNA level in ALI lung tissues significantly increased after LPS stimulation for 24 hours ( $p < 0.01$ ). Compared to the LPS group, pretreatment with low-dose inhibited the iNOS mRNA level in ALI lung tissues ( $p < 0.05$ ). Moreover, high-dose SHI group was greater than that of low-dose SHI group (Fig. 4A). In addition, after LPS stimulation for 24 hours, the mRNA level of Arg1 in ALI lung tissues increased ( $p < 0.01$ ), and pretreatment with high-dose SHI enhanced Arg1 more than the low-dose SHI group ( $p < 0.05$ ) (Fig. 4B). After LPS stimulation for 24 hours, HMGB1 mRNA level was significantly increased ( $p < 0.01$ ). Compared to the LPS group, both DXM and SHI down-regulated HMGB1 levels with the high-dose SHI group showing a greater effect than the low-dose group ( $p < 0.01$ ) (Fig. 4C). Similarly, the expression level of HMGB1 in the serum of the mice showed the same trend (Fig. 4D).

#### 3.5 The Effect of Shionone on Macrophage Polarization in RAW264.7 Cells

In this study, RAW264.7 cells were stimulated with lipopolysaccharide (LPS) as a model, and then treated with low (2  $\mu$ g/mL) or high (4  $\mu$ g/mL) doses of shionone (SHI). Shi proliferation was assessed using CCK-8 assays. Compared to the control group, LPS group was significantly reduced RAW264.7 cell proliferation ( $p < 0.01$ ). However, SHI treatment, at both low (SHI-L) and high (SHI-H) doses, significantly increased cell proliferation compared to the LPS group ( $p < 0.05$ ) (Fig. 5A). Cell morphology was observed via inverted microscopy (Fig. 5B). To investigate the effects of SHI on M1 and M2 macrophage polarization markers, iNOS and Arg1 mRNA expression in RAW264.7 cells was measured after 24 hours of LPS stimulation. LPS stimulation significantly increased iNOS mRNA levels ( $p < 0.01$ ). Pretreatment with 2  $\mu$ g/mL SHI significantly inhibited iNOS mRNA expression ( $p < 0.05$ ), and pretreatment with 4  $\mu$ g/mL SHI further inhibited iNOS mRNA levels ( $p < 0.05$ ), as shown in Fig. 5D. Similarly, LPS stimulation significantly increased Arg1 mRNA levels after 24 h ( $p < 0.01$ ). Pretreatment with 2  $\mu$ g/mL SHI significantly increased Arg1 mRNA expression ( $p < 0.05$ ), and pretreatment with 4  $\mu$ g/mL SHI further increased Arg1 mRNA levels ( $p < 0.01$ ), as shown in Fig. 5C. Immunofluorescence results indicated that SHI (2  $\mu$ g/mL and 4  $\mu$ g/mL) effectively blocked iNOS expression compared to the LPS group ( $p < 0.05$ ) (Fig. 5F,G). Additionally, 4  $\mu$ g/mL SHI enhanced Arg1 expression to a greater extent than 2  $\mu$ g/mL SHI ( $p < 0.05$ ) (Fig. 5E,H). Western blot analysis revealed that LPS stimulation significantly increased iNOS protein levels in RAW264.7 cells after 24 h ( $p < 0.01$ ). Pretreatment with 2  $\mu$ g/mL SHI for 2 hours down-regulated iNOS

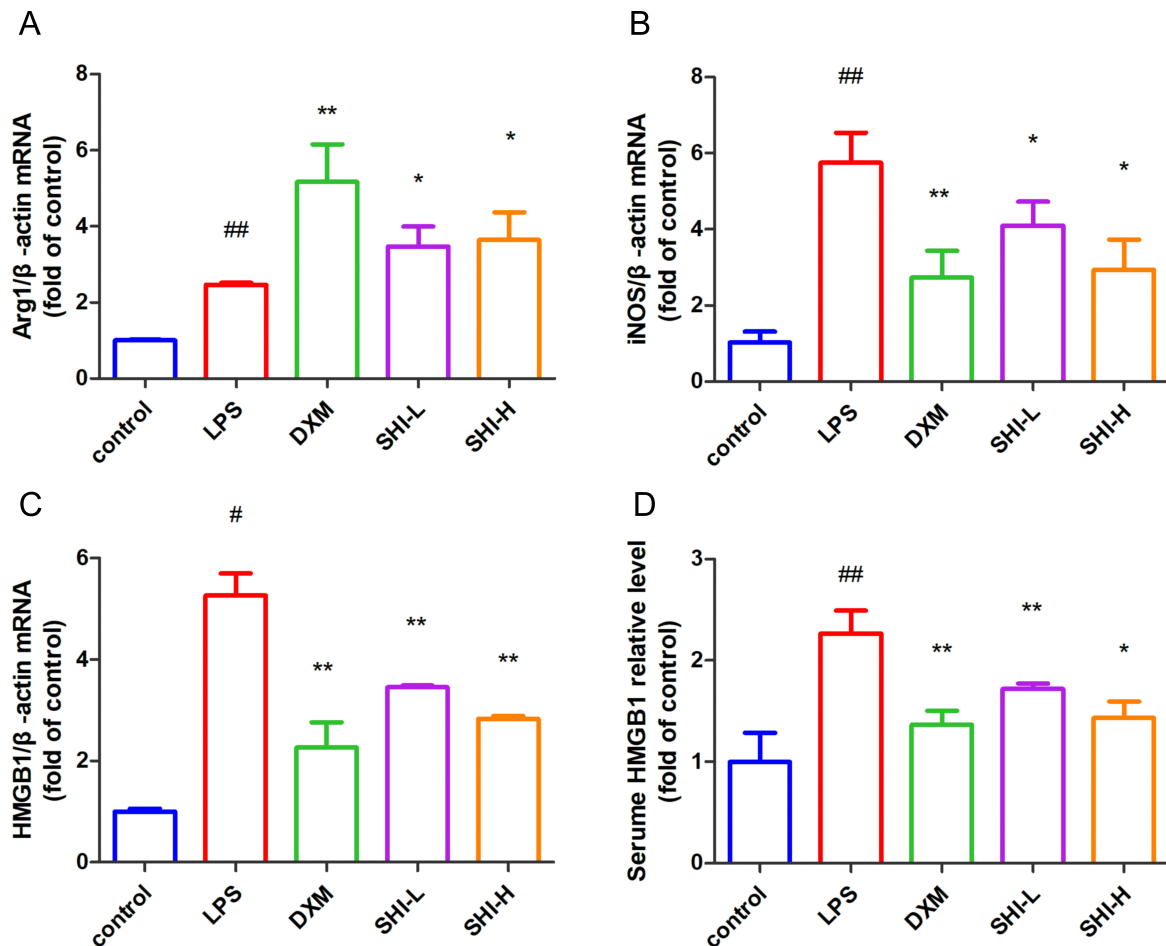


**Fig. 4. SHI affects the polarization and inhibits HMGB1 expression in ALI model lung tissue.** (A,B) mRNA expression of Arg1 and iNOS in lung tissues. (C,D) HMGB1 mRNA expression in lung tissues and serum level. Compared with the control group, # $p < 0.05$ , ## $p < 0.01$ ; compared with the LPS group, \* $p < 0.05$ , \*\* $p < 0.01$ .

protein levels ( $p < 0.05$ ), and pretreatment with 4  $\mu\text{g}/\text{mL}$  SHI for 2 hours significantly down-regulated iNOS protein levels ( $p < 0.01$ ). Concurrently, Arg1 protein levels increased after LPS stimulation ( $p < 0.01$ ). Pretreatment with 2  $\mu\text{g}/\text{mL}$  SHI increased Arg1 protein levels ( $p < 0.05$ ), and pretreatment with 4  $\mu\text{g}/\text{mL}$  SHI significantly increased Arg1 protein level ( $p < 0.01$ ) (Fig. 5I–K). The effect of SHI on lipopolysaccharide-induced inflammatory cytokines in RAW264.7 cells was also assessed by measuring the expression of TNF- $\alpha$ , IL-6, IL-1 $\beta$ , GM-CSF, IL-10 and TGF- $\beta$ 1, LPS stimulation significantly increased were measured. Results showed that levels of TNF- $\alpha$ , IL-6 and IL-1 $\beta$  significantly increased after LPS stimulation for 24 h. SHI pretreatment significantly inhibited the levels of TNF- $\alpha$ , IL-6, and IL-1 $\beta$ , and increased the levels of GM-CSF, IL-10, and TGF- $\beta$ 1 ( $p < 0.05$ ), suggesting that SHI can promote macrophage function and reduce inflammation (Fig. 5L–Q).

### 3.6 The Effect of Shionone on HMGB1/NF- $\kappa$ B Signaling in RAW264.7 Cells

To investigate whether SHI mediates macrophage polarization by regulating the HMGB1, p-NF- $\kappa$ B, and NF- $\kappa$ B signaling pathways, we examined the effect of SHI on these pathways. The results showed that SHI dose-dependently reduce the HMGB1 mRNA level in LPS-induced macrophages ( $p < 0.05$ ) (Fig. 6A). Additionally, SHI dose-dependently reduced the phosphorylation levels of HMGB1, MyD88 and p-NF- $\kappa$ B in LPS-induced macrophages ( $p < 0.05$ ) (Fig. 6B–E).

### 3.7 SHI Affects Macrophage Polarization Through HMGB1

To further investigate the role of SHI in HMGB1-mediated polarization of macrophages, we used HMGB1-siRNA to reduce HMGB1 expression in cells. We then detected the mRNA expression and protein levels of the polarization markers iNOS and Arg1 in RAW264.7 cells after 24 h of LPS stimulation. As shown in Fig. 7A–E, knocking down HMGB1 (LPS+HMGB1-siRNA group) significantly

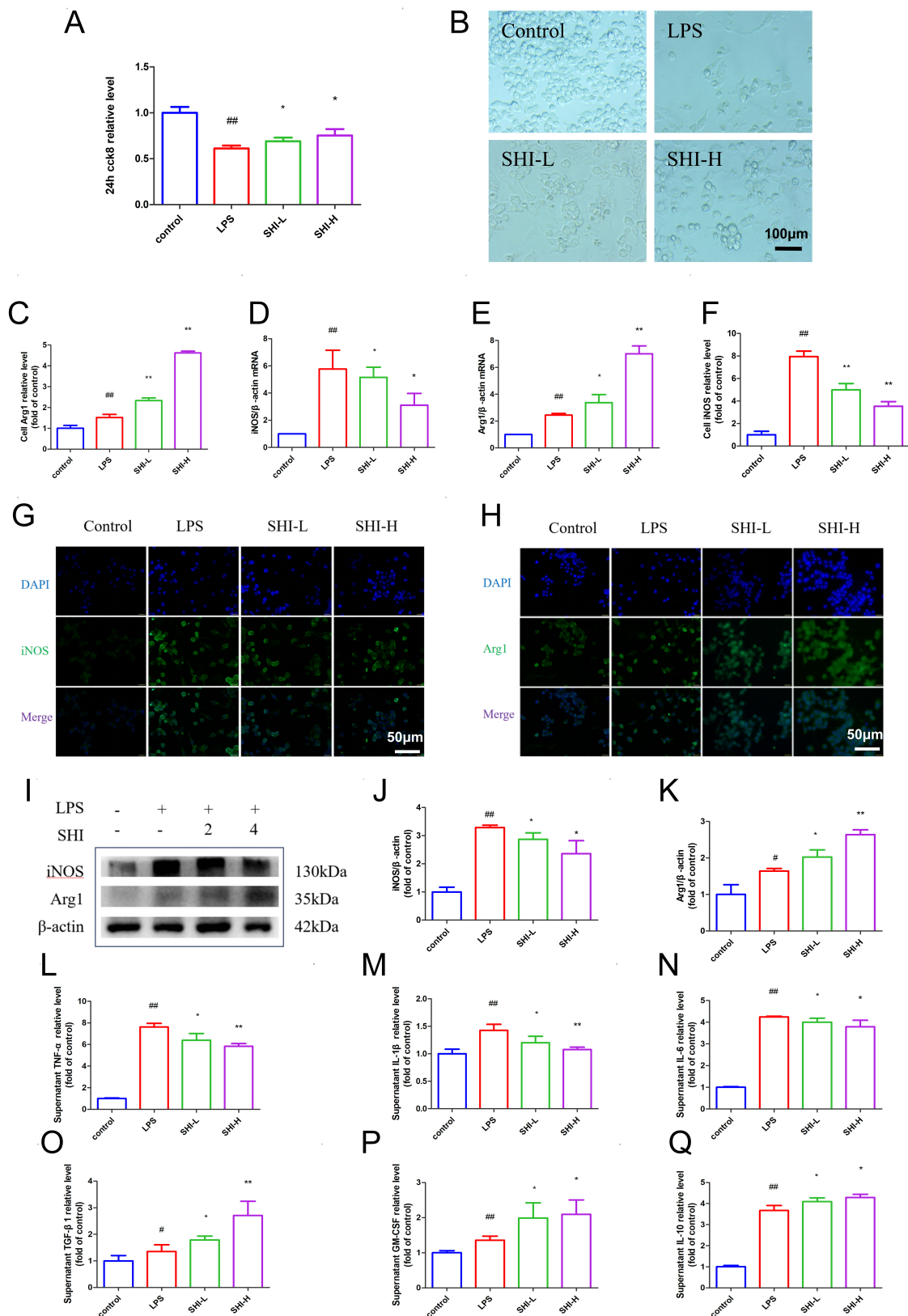


**Fig. 5. The effect of SHI on macrophage polarization.** (A) Cell Proliferation after 24 hours (CCK-8 assay). (B) Microscopic images. Scale bar: 100 μm. (C,D) Arg1 and iNOS mRNA expression in RAW264.7 cells. (E–H) Arg1 and iNOS protein expression in RAW264.7 cells by Immunofluorescence. Scale bar: 50 μm. (I–K) iNOS and Arg1 protein expression in RAW264.7 cells by Western Blot. (L–Q) TNF-α, IL-1β, IL-6, TGF-β1, GM-CSF and IL-10 expression cell culture in the supernatant. Compared with the control group, #*p* < 0.05, ##*p* < 0.01, compared with the LPS group, \**p* < 0.05, \*\**p* < 0.01.

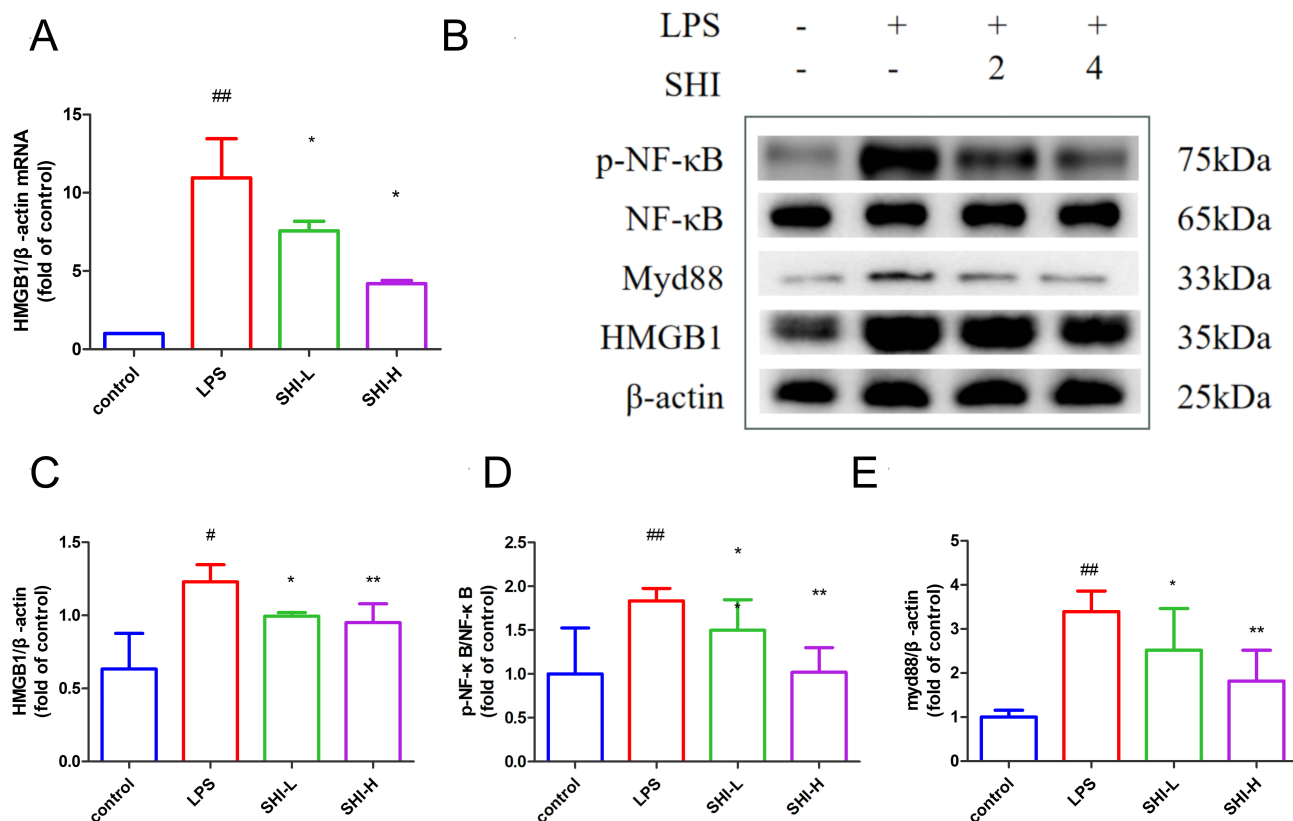


**Fig. 6. The effect of SHI on HMGB1/NF-κB signaling in RAW264.7 cells.** (A) Effect of SHI on the HMGB1 mRNA in LPS-induced RAW264.7 cells. (B–E) Protein expression of p-NF-κB, NF-κB, MyD88 and HMGB1 in cells of each group. Compared with the blank group, # $p < 0.05$ , ## $p < 0.01$ , compared with the model group, \* $p < 0.05$ , \*\* $p < 0.01$ .

inhibited the expression of iNOS ( $p < 0.05$ ) and enhanced the expression of Arg1 ( $p < 0.05$ ). As shown in Fig. 7F–K, knocking down HMGB1 significantly inhibited the expression of IL-1 $\beta$ , IL-6, TNF- $\alpha$ , GM-CSF, IL-10 and TGF- $\beta$ 1 expression in the supernatant.

### 3.8 SHI Affects Macrophage Polarization Through Regulation of the TLR4/NF-κB Pathway by HMGB1

We detected the expression of HMGB1, TLR4, MyD88, NF-κB and p-NF-κB proteins in macrophages in HMGB1-SiRNA knockdown cell lines using ELISA, IF and WB. The results showed that knocking down HMGB1 (LPS+HMGB1-siRNA group) inhibited the HMGB1-mediated TLR4/NF-κB signaling pathway ( $p < 0.05$ ), and the results were the similar to those of the LPS+SHI group ( $p < 0.05$ ) (Fig. 8A). In addition, the two treatments showed a synergistic effect ( $p < 0.05$ ), confirming that SHI affected the polarization of macrophages through the regulation of the TLR4/NF-κB pathway by HMGB1 (Fig. 8B,C). We detected the levels of related pathway proteins in RAW264.7 cells. As shown in Fig. 8E–G, HMGB1 knocked down can significantly inhibited the protein expression levels of P-NF-κB, MyD88 and HMGB1 like SHI intervention ( $p < 0.05$ ), and the two have a synergistic effect ( $p < 0.05$ ). We detected the levels of related pathway proteins

in RAW264.7 cells. As shown in Fig. 8D–G, HMGB1 knocked down can significantly inhibit the protein expression levels of p-NF-κB, MyD88 and HMGB1 similar to SHI intervention ( $p < 0.05$ ), and the two had have a synergistic effect ( $p < 0.05$ ).

## 4. Discussion

This study investigates the therapeutic mechanism by which SHI alleviates sepsis-induced ALI by regulating macrophage polarization via the HMGB1/NF-κB signaling pathway. In lipopolysaccharide-induced murine models, SHI treatment significantly mitigated lung inflammation, pulmonary edema, and histopathological damage, as evidenced by decreased lung injury scores and wet-to-dry weight ratios ( $p < 0.01$ ). Mechanistically, SHI dose-dependently suppressed M1 polarization markers while enhancing M2 polarization markers, effectively shifting the macrophage phenotype from pro-inflammatory to anti-inflammatory. This phenotypic transition was accompanied by reduced pro-inflammatory and elevated anti-inflammatory cytokines levels in both serum and lung tissues ( $p < 0.05$ ). Key mechanistic insights revealed that SHI inhibits HMGB1 expression and downstream NF-κB activation, as indicated by decreased phosphorylation of NF-κB p65, TLR4, and MyD88 ( $p < 0.05$ ). The pro-

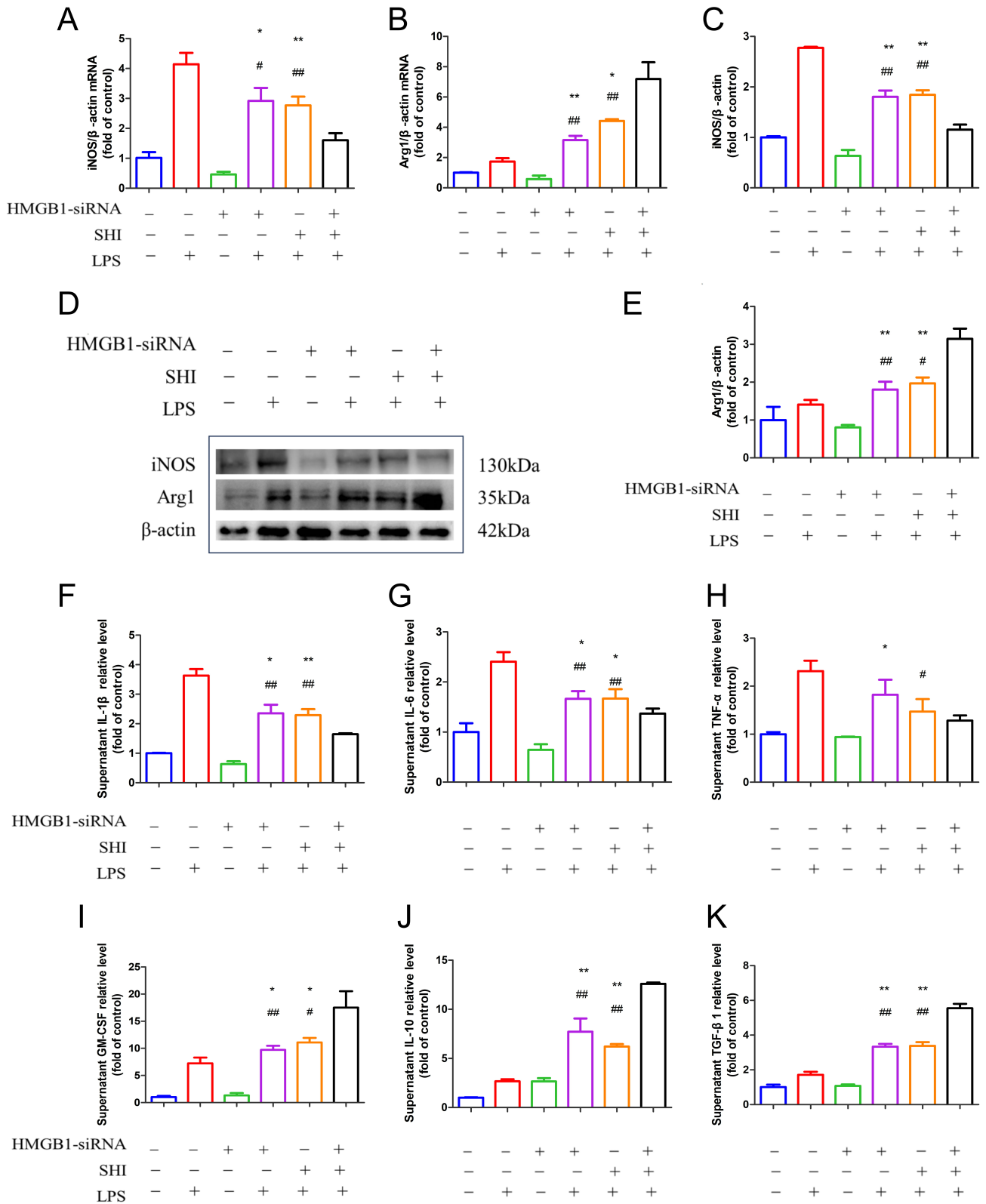


**Fig. 7. SHI affects macrophage polarization through HMGB1.** (A,B) iNOS and Arg1 mRNA expression in the RAW264.7 cells. (C–E) iNOS and Arg1 protein expression in the RAW264.7 by WB. (F–K) IL-1 $\beta$ , IL-6, TNF- $\alpha$ , GM-CSF, IL-10 and TGF- $\beta$ 1 expression in the supernatant. Compared with the LPS group, # $p$  < 0.05, ## $p$  < 0.01, compared with the LPS+HMGB1-siRNA+SHI group, \* $p$  < 0.05, \*\* $p$  < 0.01. Groups: control group, LPS group, HMGB1-siRNA group, LPS+HMGB1-siRNA group, LPS+SHI group, LPS+HMGB1-siRNA+SHI group.

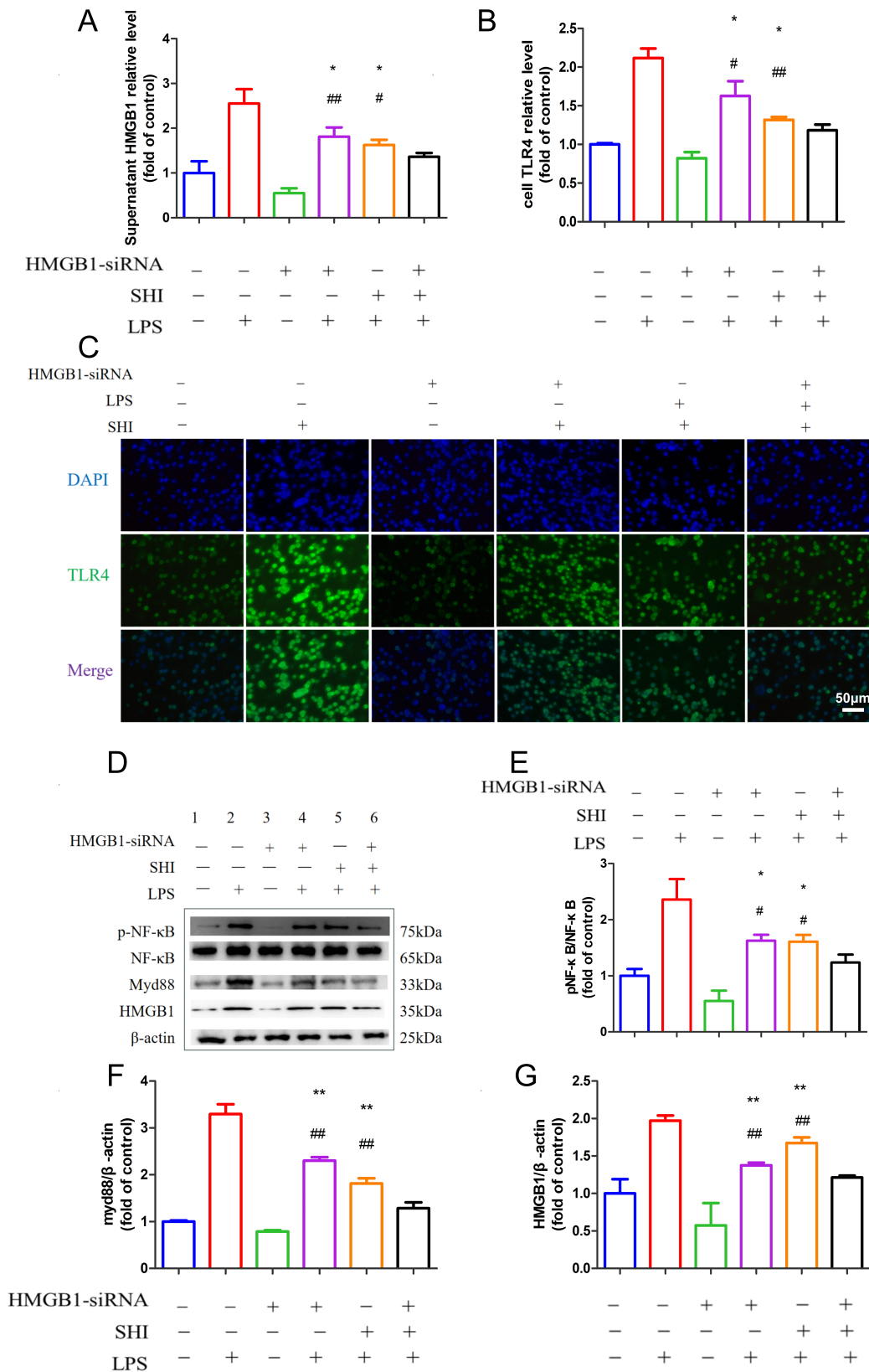


**Fig. 8. SHI affects macrophage polarization through the regulation of the TLR4/NF- $\kappa$ B pathway by HMGB1.** (A) HMGB1 expression in the supernatant. (B,C) TLR4 expression in RAW264.7 cells by IF. Scale bar: 50  $\mu$ m. (D–G) p-NF- $\kappa$ B, NF- $\kappa$ B, HMGB1, MyD88 expression in the RAW264.7 by WB. Compared with the LPS group,  $\#p < 0.05$ ,  $\#\#p < 0.01$ , compared with the LPS+HMGB1-siRNA+SHI group,  $*p < 0.05$ ,  $**p < 0.01$ . Group: control group, LPS group, HMGB1-siRNA group, LPS+HMGB1-siRNA group, LPS+SHI group, LPS+HMGB1-siRNA+SHI group.

protective effects of SHI were further validated via HMGB1 siRNA knockdown, which mimicked SHI's effects, confirming HMGB1 as a direct therapeutic target. Notably, this study advances beyond previous research [8] linking SHI to ALI mitigation via ECM1/STAT5 signaling by identifying HMGB1 as the upstream regulator of macrophage polarization. Unlike broad-spectrum NF- $\kappa$ B inhibitors, SHI selectively targets HMGB1, thereby avoiding global immune suppression while preserving M2-mediated tissue repair. These findings establish the HMGB1/NF- $\kappa$ B axis as a viable therapeutic target for sepsis-induced ALI and highlight SHI's dual role in resolving inflammation and promoting tissue recovery, providing a basis for targeted therapeutic development.

Sepsis frequently leads to multiple organ damage, with the development of a "systemic inflammatory response syndrome" impacting both humans and animals [17]. Acute lung injury, a major complication of sepsis, typically results in lung inflammation and pathological injury, significantly affecting lung pathophysiology. Sepsis can induce high concentrations of pro-inflammatory cytokines in serum and lung tissue, creating an "inflammatory storm" that further exacerbates lung damage [18]. Previous studies have reported that ECM1 serves as a critical factor required for driving M1 macrophage polarization in inflammatory bowel disease (IBD) upon LPS stimulation. [19]. This model revealed changes in lung histopathology, including inflammatory cell infiltration, alveolar wall thickening, and pulmonary edema. Drugs intervention improved these pulmonary inflammatory manifestations, indicating that SHI can be effectively reverse sepsis-induced ALI.

Sepsis alters the body's immune environment and activates macrophages, which are crucial phagocytes in the immune system distributed throughout various tissues, including the lung. Macrophages perform various functions, including pathogen phagocytosis and elimination, removal of damaged or dead cells, regulation of inflammatory responses, and promotion of tissue regeneration. Macrophage polarization is associated with the occurrence and development of immune disorders. Polarization of macrophages can lead to immune system decompensation, exacerbate the inflammatory response, and have a wide impact on the body during sepsis development [2]. Under LPS stimulation, macrophages can exhibit both pro-inflammatory and anti-inflammatory properties [20]. In the early stages of the inflammatory response, M1 macrophages activated by the classical activation via pathway, respond rapidly to infection and tissue damage by secreting various pro-inflammatory factors such as TNF- $\alpha$ , IL-6, and IL-1 $\beta$ . While appropriate inflammatory responses promote immune reactions, excessive inflammation can lead to septic shock and even death [21]. In the later stages of inflammation, M2 macrophages, activated via alternative pathways, secrete factors such as IL-10, TGF- $\beta$ 1, and GM-CSF to help repair inflammation-induced tissue damage. The

phenotype of macrophages changes with different stress conditions in the body. This balance of pro-inflammatory and anti-inflammatory phenotypes enables macrophages to respond quickly to infections and subsequently maintain homeostasis [5,21]. iNOS and Arg1 serve as well-established classical markers for M1 and M2 macrophages, respectively, respectively. Inhibition of M1 macrophages and promotion of M2 macrophages improve the survival of septic mice by promoting an anti-inflammatory response [22]. The transition from M1 phenotype to M2 phenotype demonstrates the anti-inflammatory properties of macrophages [23]. Therefore, regulating macrophage polarization represents a promising therapeutic strategy for sepsis-induced ALI.

Upon detecting danger signals, such as microbial stimulation or tissue damage, macrophages rapidly reshape themselves and activate the transcription of key downstream genes in a spatiotemporal dependent manner. This allows them to quickly and effectively perform functions such as endocytosis, phagocytosis, cytokines secretion and immune response regulation. Many studies have demonstrated that transcription regulation is crucial for macrophages polarization, and several transcription regulatory factors have been identified, including NF- $\kappa$ B. NF- $\kappa$ B is an important transcription factor involved in this process; in LPS-induced M1 polarization, the promoter regions of many M1-polarized genes, such as iNOS and MCP-1, contain NF- $\kappa$ B binding sites. LPS activates the NF- $\kappa$ B signaling pathway through Toll-like receptor 4 (TLR4), thereby promoting the production of various M1 polarization-associated cytokines [24]. As a key cytoplasmic transcription factor, NF- $\kappa$ B drives inflammatory processes and is stimulated by inflammatory mediators of tissue damage [24]. In the contexts of sepsis and ALI, NF- $\kappa$ B regulates macrophage polarization by controlling the transcription of multiple inflammatory factors [25]. In the present study, we preliminarily confirmed that the TLR4/NF- $\kappa$ B signaling pathway influences the polarization process of M1 macrophages polarization.

HMGB1 typically resides in the nucleus. Upon proper stimulation HMGB1 is either actively secreted by immune cells or passively released from necrotic or damaged cells. It translocates to the cytoplasm and acts as an initiator of the inflammatory cascade, participating in the progression of inflammatory reactions [9], exacerbating HMGB1 further exacerbates the inflammatory response, worsening patient conditions, and affecting prognosis [12]. HMGB1 binds to Toll-like receptors (TLR4,9) to activate NF- $\kappa$ B signaling and promote inflammation. HMGB1, and it can affect polarization [11]. HMGB1 plays a significant role in the NF- $\kappa$ B related pathway. Knocking out or reducing the secretion and release of HMGB1, as well as its corresponding activated forms can inhibit the subsequent inflammatory cascade, which is of great importance in the intervention of the inflammatory diseases [13]. Our study also showed that

inhibition of HMGB1 can regulate the TLR4/MyD88/NF- $\kappa$ B related pathway, down-regulate NF- $\kappa$ B phosphorylation, reduce M1 polarization, promote macrophages to M2 polarization, and inhibit inflammation. These results indicated that HMGB1 was involved in the regulation of SHI on macrophage polarization. Our analysis suggests that SHI treatment inhibits HMGB1, NF- $\kappa$ B phosphorylation, and M1 subgroup characterization, while promoting M2 expression and thereby improving lung injury in sepsis.

## 5. Limitations

This study is limited by its focus on macrophage-mediated mechanisms; future investigations should evaluate SHI's effects on other immune cell populations and explore potential crosstalk between macrophage polarization and metabolic reprogramming in sepsis.

## 6. Conclusions

Shionone mitigates sepsis-induced acute lung injury by shifting macrophage polarization from a pro-inflammatory M1 to an anti-inflammatory M2 phenotype. This therapeutic effect is achieved by suppressing the HMGB1/NF- $\kappa$ B signaling pathway, specifically through shionone's inhibition of HMGB1 release, downregulation of TLR4-MyD88 signaling, and reduction of NF- $\kappa$ B activation. These results suggest that shionone is a promising candidate for treating sepsis-associated lung injury and support targeting macrophage polarization in inflammatory lung disorders.

## Availability of Data and Materials

All data supporting the findings of this study are available within the article and are also accessible from the lead contact on request.

## Author Contributions

QW, BZ, HJ and YS designed the research study. QW and GX performed the research. QW, JZ and YL analyzed the data. QW and BZ wrote the manuscript. All authors contributed to editorial changes in the manuscript. All authors read and approved the final manuscript. All authors have participated sufficiently in the work and agreed to be accountable for all aspects of the work.

## Ethics Approval and Consent to Participate

The study was conducted in accordance with the ARRIVE guidelines. The research protocol was approved by the Ethics Committee of Suzhou Hospital of Integrated Traditional Chinese and Western Medicine (Ethic Approval Number: 2023030).

## Acknowledgment

We gratefully acknowledge the assistance and instruction from Dr. Xin Wang and professor Weiwei Tao.

## Funding

This research was supported by Jiangsu Provincial Association of Chinese Medicine Project No. CYTF2024037. Jiangsu Province Traditional Chinese Medicine Technology Development Project No. MS2023037. Suzhou Applied Basic Research (Medical and Health) Science and Technology Innovation Project No. SYWD2024333. Medical and Health Project on Suzhou Wuzhong District Science and Technology Plan Youth Project No. WZYW2023017. Applied Basic Research on Special Research of Wumenyipai with Shicaixuepai of Suzhou No. SC2023002.

## Conflict of Interest

The authors declare no conflict of interest.

## References

- [1] Barkat MQ, Li Q, Manzoor M, Xu C, Hussain N, Salawi A, *et al.* Sepsis-induced ALI/ARDS beyond supportive care: molecular mechanisms and cutting-edge therapies. *International Immunopharmacology*. 2025; 166: 115495. <https://doi.org/10.1016/j.intimp.2025.115495>.
- [2] Zhao Y, Li K, Wang L, Kuang G, Xie K, Lin S. Dexmedetomidine Mitigates Acute Lung Injury by Enhancing M2 Macrophage Polarization and Inhibiting RAGE/Caspase-11-Mediated Pyroptosis. *Frontiers in Bioscience (Landmark Edition)*. 2024; 29: 409. <https://doi.org/10.31083/j.fbi2912409>.
- [3] Song Y, Wu Q, Jiang H, Hu A, Xu L, Tan C, *et al.* The Effect of Shionone on Sepsis-Induced Acute Lung Injury by the ECM1/STAT5/NF- $\kappa$ B Pathway. *Frontiers in Pharmacology*. 2022; 12: 764247. <https://doi.org/10.3389/fphar.2021.764247>.
- [4] Murray PJ, Wynn TA. Protective and pathogenic functions of macrophage subsets. *Nature Reviews. Immunology*. 2011; 11: 723–737. <https://doi.org/10.1038/nri3073>.
- [5] Wang L, Wang D, Zhang T, Ma Y, Tong X, Fan H. The role of immunometabolism in macrophage polarization and its impact on acute lung injury/acute respiratory distress syndrome. *Frontiers in Immunology*. 2023; 14: 1117548. <https://doi.org/10.3389/fimmu.2023.1117548>.
- [6] Chen X, Tang J, Shuai W, Meng J, Feng J, Han Z. Macrophage polarization and its role in the pathogenesis of acute lung injury/acute respiratory distress syndrome. *Inflammation Research*. 2020; 69: 883–895. <https://doi.org/10.1007/s00011-020-01378-2>.
- [7] Wang Z, Wang Z. The role of macrophages polarization in sepsis-induced acute lung injury. *Frontiers in Immunology*. 2023; 14: 1209438. <https://doi.org/10.3389/fimmu.2023.1209438>.
- [8] Zhang B, Xue Y, Zhao J, Jiang H, Zhu J, Yin H, *et al.* Shionone Attenuates Sepsis-Induced Acute Kidney Injury by Regulating Macrophage Polarization via the ECM1/STAT5 Pathway. *Frontiers in Medicine*. 2022; 8: 796743. <https://doi.org/10.3389/fmed.2021.796743>.
- [9] Tang S, Xu B, Pang H, Xiao L, Mei Q, He X. Ozonated Water Inhibits Hepatocellular Carcinoma Invasion and Metastasis by Regulating the HMGB1/NF- $\kappa$ B/STAT3 Signaling Pathway. *Journal of Hepatocellular Carcinoma*. 2023; 10: 203–215. <https://doi.org/10.2147/JHC.S394074>.
- [10] Furci F, Murdaca G, Pelaia C, Imbalzano E, Pelaia G, Caminati M, *et al.* TSLP and HMGB1: Inflammatory Targets and Potential Biomarkers for Precision Medicine in Asthma and COPD. *Biomedicines*. 2023; 11: 437. <https://doi.org/10.3390/biomedicines11020437>.

- [11] Hassan NF, El-Ansary MR, Selim HMRM, Ousman MS, Khattab MS, El-Ansary MRM, *et al.* Alirocumab boosts antioxidant status and halts inflammation in rat model of sepsis-induced nephrotoxicity via modulation of Nrf2/HO-1, PCSK9/HMGB1/NF- $\kappa$ B/NLRP3 and Fractalkine/CX3CR1 hubs. *Biomedicine & Pharmacotherapy*. 2024; 177: 116929. <https://doi.org/10.1016/j.biopha.2024.116929>.
- [12] Xue J, Suarez JS, Minaai M, Li S, Gaudino G, Pass HI, *et al.* HMGB1 as a therapeutic target in disease. *Journal of Cellular Physiology*. 2021; 236: 3406–3419. <https://doi.org/10.1002/jcp.30125>.
- [13] Zhao F, Guo Z, Hou F, Fan W, Wu B, Qian Z. Magnoflorine Alleviates “M1” Polarized Macrophage-Induced Intervertebral Disc Degeneration Through Repressing the HMGB1/Myd88/NF- $\kappa$ B Pathway and NLRP3 Inflammasome. *Frontiers in Pharmacology*. 2021; 12: 701087. <https://doi.org/10.3389/fphar.2021.701087>.
- [14] Treutiger CJ, Mullins GE, Johansson ASM, Rouhiainen A, Rauvala HME, Erlandsson-Harris H, *et al.* High mobility group 1 B-box mediates activation of human endothelium. *Journal of Internal Medicine*. 2003; 254: 375–385. <https://doi.org/10.1046/j.1365-2796.2003.01204.x>.
- [15] Wang X, Yin H, Fan L, Zhou Y, Tang X, Fei X, *et al.* Shionone alleviates NLRP3 inflammasome mediated pyroptosis in interstitial cystitis injury. *International Immunopharmacology*. 2021; 90: 107132. <https://doi.org/10.1016/j.intimp.2020.107132>.
- [16] Solopov PA, Colunga Biancatelli RML, Catravas JD. Alcohol Increases Lung Angiotensin-Converting Enzyme 2 Expression and Exacerbates Severe Acute Respiratory Syndrome Coronavirus 2 Spike Protein Subunit 1-Induced Acute Lung Injury in K18-hACE2 Transgenic Mice. *The American Journal of Pathology*. 2022;192: 990–1000. <https://doi.org/10.1016/j.ajpat.2022.03.012>.
- [17] Li F, Yan R, Wu J, Han Z, Qin M, Liu C, *et al.* An Antioxidant Enzyme Therapeutic for Sepsis. *Frontiers in Bioengineering and Biotechnology*. 2021; 9: 800684. <https://doi.org/10.3389/fbioe.2021.800684>.
- [18] Ma X, Zhu G, Jiao T, Shao F. Effects of circular RNA Ttc3/miR-148a/Rcan2 axis on inflammation and oxidative stress in rats with acute kidney injury induced by sepsis. *Life Sciences*. 2021; 272: 119233. <https://doi.org/10.1016/j.lfs.2021.119233>.
- [19] Zhang Y, Li X, Luo Z, Ma L, Zhu S, Wang Z, *et al.* ECM1 is an essential factor for the determination of M1 macrophage polarization in IBD in response to LPS stimulation. *Proceedings of the National Academy of Sciences of the United States of America*. 2020; 117: 3083–3092. <https://doi.org/10.1073/pnas.1912774117>.
- [20] Locati M, Curtale G, Mantovani A. Diversity, Mechanisms, and Significance of Macrophage Plasticity. *Annual Review of Pathology*. 2020; 15: 123–147. <https://doi.org/10.1146/annurev-pathmechdis-012418-012718>.
- [21] Xu W, Hou H, Yang W, Tang W, Sun L. Immunologic role of macrophages in sepsis-induced acute liver injury. *International Immunopharmacology*. 2024; 143: 113492. <https://doi.org/10.1016/j.intimp.2024.113492>.
- [22] Odegaard JI, Chawla A. Alternative macrophage activation and metabolism. *Annual Review of Pathology*. 2011; 6: 275–297. <https://doi.org/10.1146/annurev-pathol-011110-130138>.
- [23] Liu M, Chen Y, Wang S, Zhou H, Feng D, Wei J, *et al.*  $\alpha$ -Ketoglutarate Modulates Macrophage Polarization Through Regulation of PPAR $\gamma$  Transcription and mTORC1/p70S6K Pathway to Ameliorate ALI/ARDS. *Shock*. 2020; 53: 103–113. <https://doi.org/10.1097/SHK.0000000000001333>.
- [24] Chen T, Liu S, Zheng M, Li Y, He L. The effect of geniposide on chronic unpredictable mild stress-induced depressive mice through BTK/TLR4/NF- $\kappa$ B and BDNF/TrkB signaling pathways. *Phytotherapy Research*. 2021; 35: 932–945. <https://doi.org/10.1002/ptr.6846>.
- [25] Zhang J, Wang C, Wang H, Li X, Xu J, Yu K. Loganiin alleviates sepsis-induced acute lung injury by regulating macrophage polarization and inhibiting NLRP3 inflammasome activation. *International Immunopharmacology*. 2021; 95: 107529. <https://doi.org/10.1016/j.intimp.2021.107529>.